CHROMSMP. 1449

INSIGHTS INTO THE SLURRY PACKING AND BED STRUCTURE OF CAPILLARY LIQUID CHROMATOGRAPHIC COLUMNS

DENNIS C. SHELLY*, V. L. ANTONUCCI, T. J. EDKINS and T. J. DALTON

Department of Chemistry and Chemical Engineering, Stevens Institute of Technology, Hoboken, NJ 07030 (U.S.A.)

SUMMARY

New techniques have been developed for studying filtration phenomena and packing structure in slurry-packed fused-silica microcolumns. Filtration was studied by direct measurement of packing pressure, flow-rate, bed height and time using a computer-interfaced packing apparatus. Optical microscopy methods and image analysis techniques were used to study packing structure. These results plus chromatographic figures of merit were combined in order to learn more about the packing process and its relationship to chromatographic performance.

INTRODUCTION

Fused-silica microcolumns have recently been used to study the slurry-packing technique. Shelly and Edkins[1] have identified some of the unique features of these columns which influence the way in which they are packed and a novel method by which the packing process can be studied. The reproducible preparation of stable, efficient fused-silica microcolumns packed with 5-μm reversed-phase material[2] and various polar bonded phases[3] has been reported. In the papers cited, details of the slurry and pump solvent choices, nature of the pressure–time profile and post-packing conditioning schemes were given. Verzele *et al.*[4] examined some new aspects of slurry packing, such as particle shape and size effects. A comprehensive review of microcolumn technology was presented by Novotny[5]. The packing of several types of "microscale" columns was described by Ishii *et al.*[6].

Despite these advances, the reproducible preparation of efficient and stable microcolumns containing 3-μm and smaller particles remains elusive. We have attempted to develop an improved understanding of slurry packing, especially the packing of 3-μm octadecylsilane (ODS)-bonded particles, using an array of techniques and concepts from several technologies. Slurry packing can be viewed as a complex process involving three distinct phenomena: (a) colloid chemistry, (b) slurry rheology and (c) particle filtration[1]. When slurries have a low solids content, rheological effects tend to be minimal. However, colloid chemistry (interfacial tension and electrostatics) and particle filtration are critically important to the preparation of good chromatographic beds (filter cakes)[1]. A tetrahydrofuran–methanol slurry–packing solvent combination, followed by water conditioning, yields very stable fused-silica micro-

columns with a performance reproducibility of 1.33% (relative standard deviation on the minimum reduced plate height, h_{min}, where $h_{min} = 4.8$)[1]. In an effort to obtain more efficient columns, we have focused on particle filtration and the resulting bed structure associated with our approach to slurry packing. Recently, Hoffman and Blomberg[7] suggested that filtration, influenced by slurry density, is particularly important in the packing of 3-μm particles.

This paper deals explicitly with our efforts to understand particle filtration and structural effects of the fused-silica microcolumn chromatographic beds. Our first objective was to develop a fully instrumented packing apparatus with which we could control and measure pressure, flow-rate, bed-height and time during packing. The development of novel bed visualization techniques was our second objective. Our third objective was to identify those unique material properties which are fundamentally important to the packing process. These studies are a logical extension of our previous attempts[1] to develop an improved understanding of the packing of 3-μm particles in fused-silica microcolumns.

EXPERIMENTAL

Computer-controlled pump

An ISCO (Lincoln, NE, U.S.A.) μLC-500 syringe pump was interfaced to a Leading Edge (Canton, MA, U.S.A.) Model D computer using a Model INST 54 analog-to-digital interface (Cyber Research, New Haven, CT, U.S.A.). The computer was equipped with version 3.10 of MS-DOS and version 3.11 of BASIC. A Model DT707 screw terminal panel (Data Translation, Marlboro, MA, U.S.A.) was used to connect the interface to the pump via a 3-m long shielded cable.

A BASIC program (*ca.* 950 lines) was written for pump control and monitoring. The pump was operated in the controlled-pressure mode in which the pressure–time relationship was defined by any of three options: linear, logarithmic or a logarithmically-modified linear. Pressure, flow-rate and time were stored to disk during a pressurization cycle. All packing experiments began at atmospheric pressure and proceeded to a defined pressure. For the linear profile, the slope of the curve, in p.s.i./s, was selected in addition to the final pressure. For the logarithmic profile, the pressure (P)–time (t) relationship was defined by $P = a(t^{3/2} - t^{6/5})$, where $1.0 < a < 1.15$ and a was user-selectable. This function and the values of a were chosen from extensive modeling of a desired logarithmic pressure *vs.* time profile that would allow a maximum pressure to be achieved in about 15 min. The logarithmically modified linear profile was implemented by beginning with a linear profile (with a selectable slope) and converting to a logarithmic profile (using the relationship described above) at the desired switch-over pressure. Thus, three variables were selected for this option: slope, a and switch pressure. Three consecutive analog-to-digital conversions were averaged for each stored pressure and flow-rate data point. After pressurization, a monitoring period of varibable duration could be implemented. All stored data could be restored and displayed in tabular form or as pressure *vs.* time and flow-rate *vs.* time plots. Other features included pump stop and start, automatic shutdown at over-pressure (9500 p.s.i.) and pressure transducer compensation control.

Bed visualization measurements

A photographic enlarger–mask combination was developed to visualize sections of packed fused-silica microcolumns. The mask was fabricated by means of photographic techniques and standard laboratory hardware. Fig. 1 shows a line drawing of the mask design. The mask image was defined from a 1.4 mm wide line, photographically reproduced on to Kodalith negative film (Eastman Kodak, Rochester, NY, U.S.A.), resulting in an average line width of 0.2 mm. Four strips of paper tape were positioned as shown in order to form a channel in which the fused-silica microcolumn would be reproducibly positioned in the mask opening. The mask was attached to a frame-type film holder, supplied with the enlarger.

A Model 67C enlarger (Charles Beseler, Florham Park, NJ, U.S.A.) was controlled by a Model 300 darkroom timer (DIMCO*Gray, Dayton, OH, U.S.A.). A mask was used to isolate light from a 0.2 mm wide, 35 mm long portion of the column. Each segment was enlarged to 0.9 mm wide and 225 mm long. Black-and-white photographic paper (Eastman Kodak) and a No. 2 contrast enhancement filter (Ilford, Cheshire, U.K.) were used to produce the prints. A 12 ± 0.5 s exposure time (aperture $= f/8$) was used for each segment. Translation from one column segment to the next was accomplished by partially releasing tension in the mask–frame sandwich and pulling the column through in 35 ± 3 mm portions. Prior to visualization, each column was flushed with acetonitrile followed by carbon tetrachloride, the latter being used as a refractive index matching liquid.

Material properties studies

A series of experiments that compared material properties of two commercial packings were designed. Two commonly used spherical 3-μm ODS packings were chosen: Spherisorb ODS-2 (Lot 26/79) and Hypersil (Lots 1743 and 11 1383). Both were obtained from Keystone Scientific (State College, PA, U.S.A.).

Specific gravity measurements. Moore/van Slyke specific gravity bottles (National Glass and Plastic, Camden, NJ, U.S.A.) were used for both solvents and slurries. After the specific gravity of solvent alone (tetrahydrofuran, THF) and of the solvent + particles had been determined, the specific gravity of the particles was calculated by difference. THF was chosen because the particles approximate defloculated behavior when suspended in this solvent, thus minimizing errors caused by air entrapment or non-uniform wetting during agglomeration.

Sediment quotient study. A sediment quotient study[1] was performed in order to obtain the settling tendencies of the materials. The solids content was 120 mg/ml, representing the actural slurry concentration used when packing a fused-silica microcolumn.

Interfacial tension measurements. The technique described by Absolom and Barford[8] was used, except that the 1-propanol–water mixtures spanned the surface tension range 25–31 mJ/m². For each of the packing materials, 160 mg were suspended in 400 μl of solvent (400 mg/ml). All slurries were degassed, sonicated and then transferred to settling tubes. Surface tension measurements of the solvent were performed with a Kruss (Hamburg, F.R.G.) Interfacial-Tensiometer K8. Final sediment quotient measurements were obtained after a 24–48-h settling time.
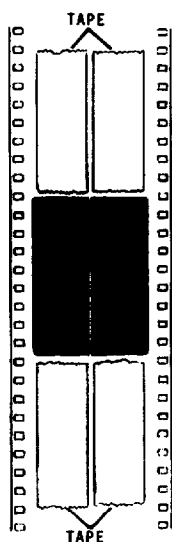
TAPE

TAPE

Fig. 1. Mask design.

On-column injector

    A new on-column injector was fabricated which permitted convenient, dispersion-free sample injections. A modified stopped-flow technique[9,10] was used in which the top 2–3 mm of the column contained the sample, introduced using a micro-plunger. The details of this device will be given in a separate publication.

Chemicals and reagents

    High-performance liquid chromatography-grade solvents (Burdick & Jackson, Muskegon, MI, U.S.A.) were used for all packing, slurry and elution solvents. All photographic chemicals (Eastman Kodak) were prepared and used according to manufacturer's directions. The column test mixture has been described previously[1]. Details of the column fabrication, including the fused-silica capillaries (Polymicro Technology, Phoenix, AZ, U.S.A.) and epoxy (Epoxy Technology, Billerica, MA, U.S.A.) that were used, has been described[1,11].

RESULTS AND DISCUSSION

Computer-controlled packing

    Linear packing profile. The computer-controlled pump was used to pack fused-silica microcolumns, simultaneously storing pressure, flow-rate and time data for subsequent analysis.

    Column 1 was packed using a linear pressurization profile with a slope of 19 p.s.i./s. Fig. 2A shows the pressure *vs.* time plot and Fig. 2B shows the flow-rate *vs.* time plot for the preparation of column 1. As pressure was the control parameter, we would expect the profile in Fig. 2A. The profile in Fig. 2B is also expected in that there is initially a high flow-rate, corresponding to slurry flowing to meet the frit, followed by a dramatic decrease in flow-rate as the bed begins to form. A steadily decreasing
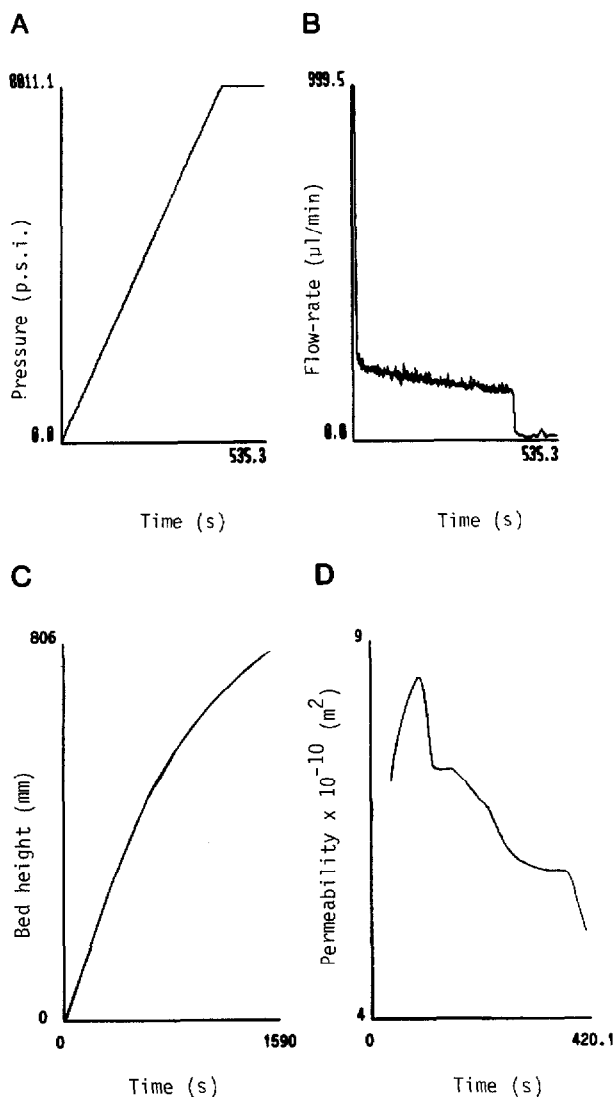
A

B

C

D

Fig. 2. Linear profile packing data. A, Pressure *versus* time plot; B, flow-rate *versus* time plot; C, bed-height *versus* time plot; D, permeability *versus* time plot.

flow-rate is seen, which indicates increasing resistance from a continuously increasing bed length. At 8000 p.s.i., the pressure remained constant, which explains the plateau in Fig. 2A and the drop in flow-rate in Fig. 2B. The bed height was recorded (manually) every 30 s by marking a length of tape, attached along the edge of a meter stick, which was placed next to the column. Fig. 2C shows a plot of bed height or length *vs.* time for the entire length of the column. The column required 1590 s to pack, hence approximately one third of the column was packed during the period indicated in Fig. 2A and B. Note that the bed height profile is not linear, especially over the last 300 mm.

It is reasonable to expect that the packing density in that region would be different from that in the rest of the column.

Integration of all the data can yield useful information concerning the permeability of the column. Bristow and Knox[12] gave two equations, which have a common variable, t_0. Eqn. 1 defines the total porosity, ε_T:

$$\varepsilon_T = \frac{4 f_v t_0}{\pi d_c^2 L} \tag{1}$$

where f_v is the volumetric flow-rate, t_0 is the void time, d_c is the column diameter and L is the column length. Eqn. 2 relates the specific column permeability, K^0, in terms of measurable parameters:

$$K^0 = \frac{\eta L^2}{\Delta p\, t_0} \tag{2}$$

where η is the mobile phase viscosity and Δp is the pressure differential. Solving both equations for t_0, setting them equal to each other and rearranging gives

$$\varepsilon_T K^0 = \frac{4 \eta f_v L}{\pi d_c^2 \Delta p} \tag{3}$$

According to Cramers *et al.*[13], K^0 is equal to $K/(\varepsilon_u + \varepsilon_i)$, where K is the bed permeability and ε_u and ε_i are the inter- and intra-particle porosities, respectively. Considering that $\varepsilon_T = \varepsilon_u + \varepsilon_i$, the left-hand side of eqn. 3 is simply K, the bed permeability. Using this information, we calculated permeability at several intervals, up to 8000 p.s.i., from the data shown in Fig. 2A, B and C. These results are shown in Fig. 2D. A predictable trend towards lower permeability with increasing time is shown in this plot. As yet, we have no adequate explanation for the steep rise in permeability in the first 100 s of the plot. Fluctuations in the flow-rate measurements could have caused some of the features of the plot. Two assumptions must hold for our approach to be valid, *i.e.*, that the measured system pressures and system flow-rates are solely attributable to the chromatographic bed. Any other contributions, such as clogging of the slurry reservoir or column, would introduce significant errors.

Logarithmic packing profile. By means of the computer-interfaced pump, another column was packed, using a logarithmic profile. Column 2 was packed using the logarithmic pressure–time profile with $a = 1.15$ and a final pressure of 8000 p.s.i. Fig. 3A, B, C and D show the same type of data, corresponding to column 1 and Fig. 2. The differences in Figs. 2 and 3 are remarkable. Fig. 3B shows an increasing flow-rate after the initial surge, attributable to the increasingly more rapid rate of pressurization as the pressure approaches 8000 p.s.i. However, there is a distinct flattening of the flow-rate curve as the pressure approaches the maximum. In Fig. 3C, there is greater linearity in the bed height–time profile than in Fig. 2C. Nonetheless, 2388 s were required to pack column 2. The differences indicated in Fig. 3B and C, compared with the same data in Fig. 2, could imply that the longitudinal uniformity of the packing density of the two columns would be very different. As in Fig. 2D, we calculated the

permeability at several intervals, using the data from Fig. 3A, B and C. Fig. 3D shows a shape that is very different from that in Fig. 2D. There is relatively constant permeability in the logarithmically packed column. This may suggest that the formation of the first few centimeters of the column dramatically affects the formation kinetics of the remainder of the bed. The filtration rate for the first 5 cm of column 2 was nearly half that for column 1. Hence the slope of the pressure–time profile influences the packing kinetics of the bed.

Column evaluation. The chromatographic performance of the two columns was evaluated as in a previous study[1]. Fig. 4 shows Van Deemter and Knox plots for both
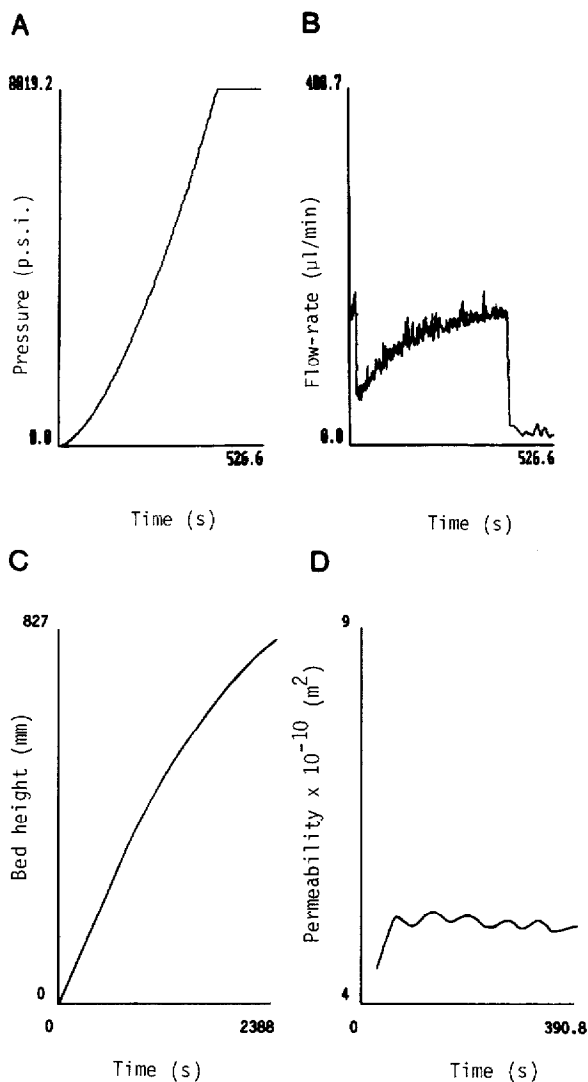
A

8819.2

Pressure (p.s.i.)

0.0

526.6

Time (s)

B

408.7

Flow-rate (µl/min)

0.0

526.6

Time (s)

C

827

Bed height (mm)

0

0   2388

Time (s)

D

9

Permeability $\times$ 10^{-10} (m^2)

4

0   390.8

Time (s)

Fig. 3. Logarithmic profile packing data. A, Pressure *versus* time plot; B, flow-rate *versus* time plot; C, bed-height *versus* time plot; D, permeability *versus* time plot.

A

LINEAR VELOCITY, mm/s
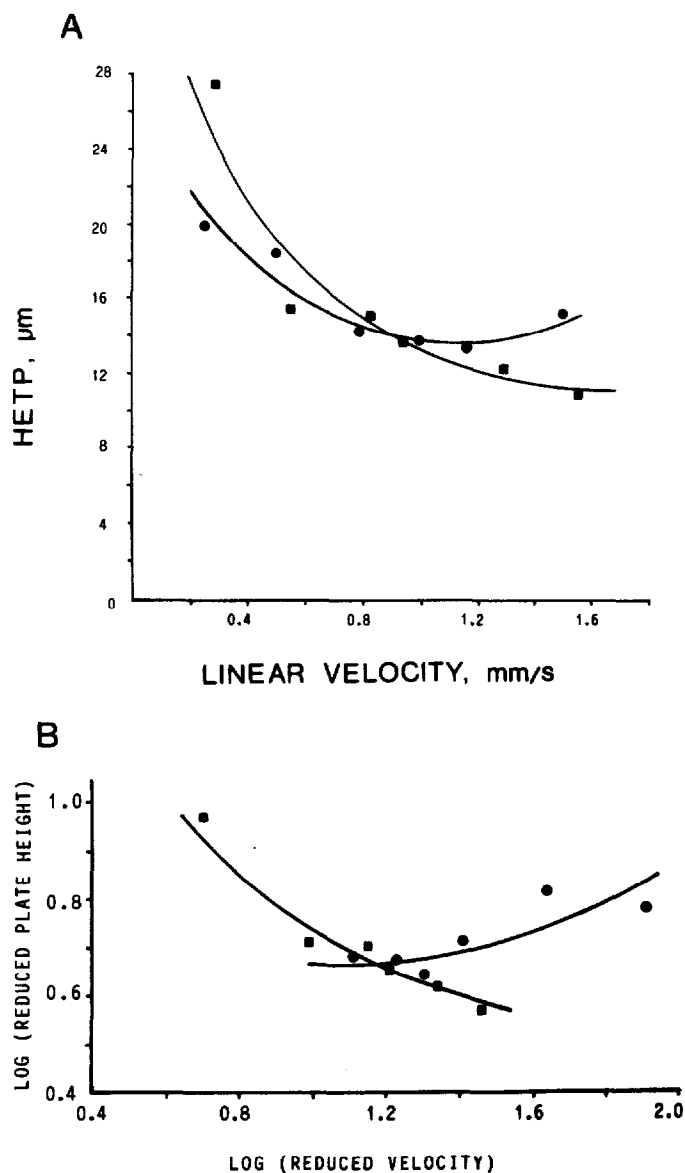
B

LOG (REDUCED VELOCITY)

Fig. 4. Column performance analysis. ● = column 1, linear packing profile; ■ = column 2, logarithmic packing profile. A, Van Deemter plot; B, Knox plot.

columns. The linear column seems to display a fairly typical kinetic performance. However, the logarithic column shows significant longitudinal dispersion contributions and no distinct minima in either plot. Other pertinent performance data are listed in Table I. It can be seen from these data that the two columns are roughly equivalent, except for their optimal efficiencies. These results are the best we have obtained for 3-μm materials, but it is possible that Spherisorb material (this study) produces slightly

TABLE I

COLUMN PERFORMANCE DATA

Column	h_{min}	$K^0 \cdot 10^{-10}$ (cm^2)	ε_T	φ	E
1	4.45	‚ 1.49	0.94	602	11954
2	3.67	1.54	0.98	584	7886

more efficient columns than Hypersil material (see ref. 1). We suspect that our void volume marker is partly retained, hence the ε_T values are unusually high. However, lower t_0 values would also decrease the flow resistance factor, φ, and the separation impedance, E, and increase K^0. We observed no changes in bed height during column evaluation with the new on-column injector design. However, during repeated injections at 1000 p.s.i. some movement of the bed (in both columns) was noted.

Bed visualization measurements

The packing or bed structure of a chromatographic column has rarely been studied in a direct fashion. However, fluidized beds have been studied photo-graphically with respect to mass transport[14] and phase structure[15]. Electron microscopy has been employed to illustrate the differences in packing columns with flocculated and deflocculated slurries[1]. Although this technique affords excellent resolution, the destructive nature of the sampling cannot be avoided. We have been pursuing the development of non-destructive techniques for viewing the particle packing structure of packed columns. Fused-silica microcolumns are an ideal test structure because of optical transparency, mechanical stability and ease of manipula-tion and handling. It is well known that the optical density of a packed bed changes, depending on the difference in refractive index of the mobile phase relative to that of the packing material. Hence it should be possible to observe directly differences in packing density by properly matching refractive indices and measuring a refractive-index-specific parameter, such as optical density.

Preliminary results from several experiments are presented here. Fig. 5 shows the projections of four segments from column 1. Keeping in mind that the segment from 70 to 105 mm was packed in the linear (constant filtration rate) portion of Fig. 2C and the segment extending from 735 to 770 mm was packed in a region of decreasing filtration rate, it is apparent that the optical differences in segments A and D are due to differences in filtration rate. As the mask–projection apparatus functions like a negative, the darker the image, the lighter is the exposure. Hence, more light propagates through the column in segment A than in segment D, primarily owing to a greater packing density in segment D than in segment A. Segment B shows the presence of bubbles, which completely disrupted the bed. This occurred although both ends were completely sealed with epoxy resin and despite the fact that this segment is approximately in the middle of the column. The mere presence of a bubble, under these conditions, may be indicative of mechanical stresses on the bed in this region of the column. Little direct evidence of the mechanical stability of packed fused-silica microcolumns is available from the literature. Segment C is darker than segment D, implying that a gradation of optical density and packing density occurs, roughly
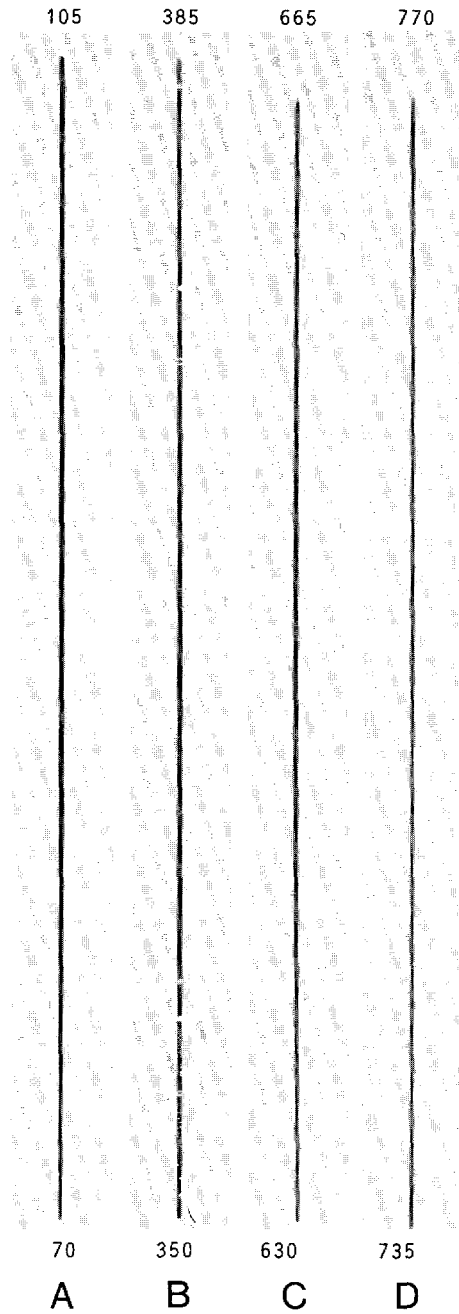
Fig. 5. Column projections for column 1, linear packing profile. A, 70–105 mm segment; B, 350–385 mm segment; C, 630–665 mm segment; D, 735–770 mm segment.

corresponding to the profile in Fig. 2A. The exposure-to-exposure reproducibility of the technique was very good. The positioning reproducibility of the technique was not as good, primarily owing to the inability to position the column accurately, because the column was not marked in any way along its length. However, the positioning accuracy within the mask was fairly good, as evidenced by the fact that segments A and B are similarly dark, yet separated by more than 200 mm. Bed structure, as evidenced by particle density, relates to porosity of the bed in a fairly straightforward manner. However, particle density relates to bed permeability in a more complex fashion. The data in Fig. 5 should be interpreted in this context. Unfortunately, column 2 could not be examined using this technique because its bed structure was accidently disrupted after the column evaluation studies.

Material property studies

Specific gravity measurements. Moore/van Slyke bottles were used to measure the specific gravity (ρ) of the solvent (THF), yielding excellent agreement with literature values ($\rho_{lit.}$ = 0.889, $\rho_{expt.}$ = 0.883 at 20°C)[16]. Although these bottles are routinely used for liquids, we also obtained reliable results for slurries. A value of 1.63 g/ml was measured for the Hypersil material compared with a value of 1.69 g/ml for the 3-μm Spherisorb. Based on a duplicate of Spherisorb, the precision was estimated to be better than 0.5%, indicating that there is a significant difference in their specific gravities. These results are in agreement with a previous report[7] in which a balanced-density technique was employed to pack 3-μm particles.

Sediment quotient study. Fig. 6A is a bar graph of sediment quotients (SQ) for two lots of Hypersil and one lot of Spherisorb. For both materials, methanol gave a higher SQ than THF. This is to be expected because methanol slurries exhibit flocculated properties and THF slurries show nearly deflocculated behavior[1]. It is important to note that the THF–Spherisorb slurry (bar C) gave a lower SQ than THF–Hypersil (bars A and B), because columns packed with Spherisorb have given better efficiencies than Hypersil-packed columns[17], indicating that there may be a relationship between extent of deflocculation and ultimate chromatographic efficiency.

Interfacial tension measurements. As indicated in Fig. 6B, both particle types gave identical interfacial tension (γ) results (γ = 27.5 mJ/m^2) although, as noted in the sediment quotient study, the absolute SQ values were different. A local maximum is reached at 27.5 mJ/m^2 and the curves steeply approach an SQ of 1000 as the interfacial tension extends beyond 28.25 mJ/m^2. This sharp increase is due to the vanishing wettability of the particles, which results in air and solvent bubbles becoming trapped in the particle aggregates. These data (Fig. 6B) also reflect the decreasing wettability of the reversed-phase packing by an increasingly aqueous medium. There may also be surface area and shape dependences on the measured interfacial tension, as our data for 3-μm spherical particles are much lower than for 5-μm irregular materials[8,18]. Our data suggest that the different sediment quotient values would appear to be related to differences in particle density rather than interfacial tension. Studies are in progress to confirm this relationship.
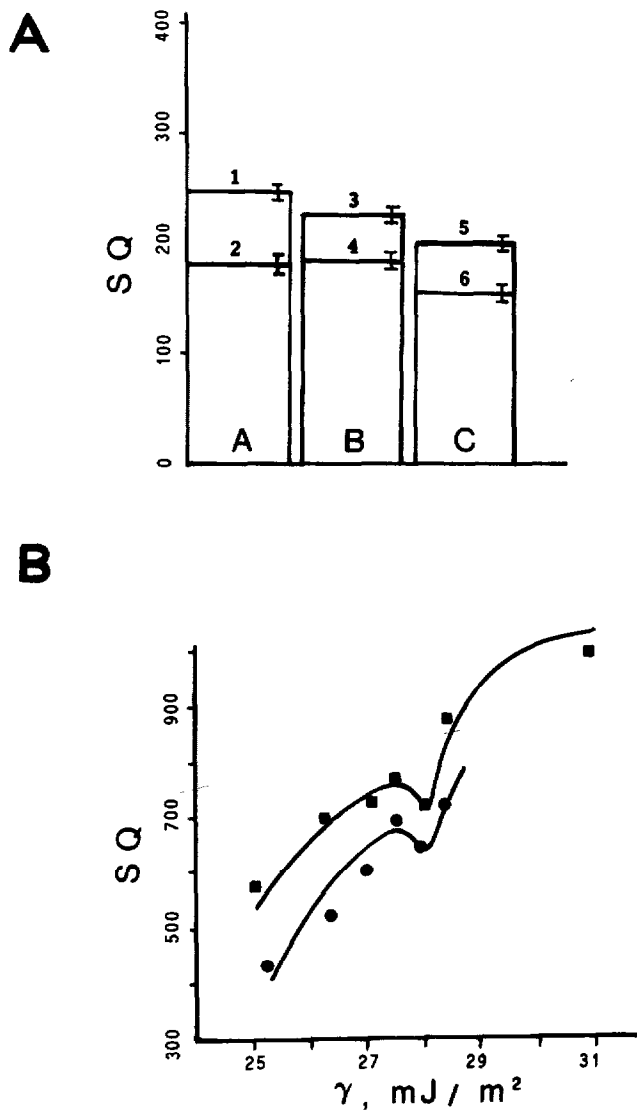
Fig. 6. Data on materials properties for 3-μm packings. A, Sediment quotient study. Section A, Shandon Hypersil ODS, Lot 1743; 1, methanol slurry; 2, tetrahydrofuran slurry. Section B: Shandon Hypersil ODS, Lot 11 1383: 3, methanol slurry; 4, tetrahydrofuran slurry. Section C: Spherisorb ODS2, Lot 26/79: 5, methanol slurry; 6, tetrahydrofuran slurry. B, Interfacial tension measurements ■ = Shandon Hypersil ODS, Lot 11 1383; ● = Spherisorb ODS 2, Lot 26/79.

CONCLUSIONS

Several important conclusions can be formulated from our work. First, more details of particle filtration, as a component of slurry packing, have been revealed. Constant-rate filtration appears to be very important, mainly to the extent of assuring

longitudinal uniformity of the packing density. The rate of filtration is also important, as evidenced by slightly lower reduced plate heights for the logarithmic profile packed column, which packed more slowly than the linear profile column. A lower slurry density should accomplish the same objective in a shorter time. Second, we have obtained direct evidence of a relationship between particle filtration rate and packing density. It appears that the faster the bed forms, the looser is the packing structure. To confirm this, we should have packed columns under the same kinetic constaints, *i.e.*, allowing the pressure to reach 8000 p.s.i. after 15 min for both the linear and logarithmic profiles. Third, a more complete description of slurry packing is emerging, a picture which contains three major components: colloid chemistry, slurry rheology and particle filtration. A unifying element in this description is basic materials properties, which can be used to explain why the particles behave as they do under various conditions. As we learn more about the materials aspects of chromatographic particles, we shall be better prepared to design and implement new column structures.

REFERENCES

1　D. C. Shelly and T. J. Edkins, *J. Chromatogr.*, 411 (1987) 185.
2　C. Borra, S. M. Han and M. Novotny, *J. Chromatogr.*, 385 (1987) 75.
3　F. Andreolini, C. Borra and M. Novotny, *Anal. Chem.*, 59 (1987) 2428.
4　M. Verzele, C. Dewaele and D. Duquet, *J. Chromatogr.*, 391 (1987) 111.
5　M. Novotny, *Anal. Chem.*, 60 (1988) 500A.
6　D. Ishii, T. Takeuchi and A. Wada, in D. Ishii (Editor), *Introduction to Microscale High-Performance Liquid Chromatography*, VCH, New York, NY, 1988, Ch. 3, pp. 33–67.
7　S. Hoffmann and L. Blomberg, *Chromatographia*, 24 (1987) 417.
8　D. R. Absolom and R. A. Barford, *Anal. Chem.*, 60 (1988) 210.
9　Y. Hirata and M. Novotný, *J. Chromatogr.*, 186 (1979) 521.
10　Y. Hirata and K. Jinno, *J. High Resolut. Chromatogr. Chromatogr. Commun.*, 6 (1983) 196.
11　D. C. Shelly, J. C. Gluckman and M. V. Novotny, *Anal. Chem.*, 56 (1984) 2990.
12　P. A. Bristow and J. H. Knox, *Chromatographia*, 10 (1977) 279.
13　C. A. Cramers, J. A. Rijks and C. P. M. Schutjes, *Chromatographia*, 14 (1981) 439.
14　L. Massimilla and J. W. Westwater, *AIChE J.*, 6 (1960) 134.
15　P. L. Yue, L. Rizzuti and V. Augugliaro, *Chem. Eng. Sci.*, 41 (1986) 171.
16　R. C. Weast (Editor), *CRC Handbook of Chemistry and Physics*, CRC Press, Cleveland, OH, 54th ed., 1973, p. C306.
17　T. J. Edkins and D. C. Shelly, unpublished results, 1988.
18　R. A. Barford, personal communication, 1988.